PROCEEDINGS OF SPIE

SPIEDigitalLibrary.org/conference-proceedings-of-spie

Lung deformation between preoperative CT and intraoperative CBCT for thoracoscopic surgery: a case study

Pablo Alvarez, Matthieu Chabanas, Simon Rouzé, Miguel Castro, Yohan Payan, et al.

Pablo Alvarez, Matthieu Chabanas, Simon Rouzé, Miguel Castro, Yohan Payan, Jean-Louis Dillenseger, "Lung deformation between preoperative CT and intraoperative CBCT for thoracoscopic surgery: a case study," Proc. SPIE 10576, Medical Imaging 2018: Image-Guided Procedures, Robotic Interventions, and Modeling, 105761D (13 March 2018); doi: 10.1117/12.2293938

SPIE.

Event: SPIE Medical Imaging, 2018, Houston, Texas, United States

Lung deformation between preoperative CT and intraoperative CBCT for Thoracoscopic Surgery: a case study

Pablo Alvarez[a,b], Matthieu Chabanas[b], Simon Rouzé[a,c], Miguel Castro[a], Yohan Payan[b], and Jean-Louis Dillenseger[a]

[a]INSERM, U1099, Rennes, France; Université de Rennes 1, LTSI, Rennes, France
[b]Univ. Grenoble Alpes, CNRS, Grenoble-INP, TIMC-IMAG; Grenoble, France
[c]CHU Rennes, Service de chirurgie thoracique cardiaque et vasculaire, Rennes, France

ABSTRACT

Video-Assisted Thoracoscopic Surgery (VATS) is a promising surgical treatment for early-stage lung cancer. With respect to standard thoracotomy, it is less invasive and provides better and faster patient recovery. However, a main issue is the accurate localization of small, subsolid nodules. While intraoperative Cone-Beam CT (CBCT) images can be acquired, they cannot be directly compared with preoperative CT images due to very large lung deformations occurring before and during surgery. This paper focuses on the quantification of deformations due to the change of positioning of the patient, from supine during CT acquisition to lateral decubitus in the operating room. A method is first introduced to segment the lung cavity in both CT and CBCT. The images are then registered in three steps: an initial alignment, followed by rigid registration and finally non-rigid registration, from which deformations are measured. Accuracy of the registration is quantified based on the Target Registration Error (TRE) between paired anatomical landmarks. Results of the registration process are on the order of 1.01 mm in median, with minimum and maximum errors 0.35 mm and 2.34 mm. Deformations on the parenchyma were mesured to be up to 14 mm and approximately 7 mm in average for the whole lung structure. While this study is only a first step towards image-guided therapy, it highlights the importance of accounting for lung deformation between preoperative and intraoperative images, which is crucial for the intraoperative nodule localization.

Keywords: Video Assisted Thoracoscopic Surgery (VATS), Image Registration, Lung, Cone-Beam CT

1. INTRODUCTION

Lung cancer remains as the worldwide leading cause of cancer death for both women and men.[1,2] Such a high mortality is related to the late detection of the disease, where curative treatements are normally not available and the 5-year survival rate lies between 6% and 18%.[2,3] However, screening programs performed on patients at risk have demonstrated that survival rates might be significantly increased if diagnosis and treatement are performed at early stages.[4,5] In such scenarios, surgical resection of malignant nodules is prescribed to patients. The treatement is performed via either open thoracotomy or video-assisted thoracoscopic surgery (VATS), the latter being the least invasive method with better and faster patient recovery.[6]

Even if preoperative CT images are used for planning VATS intervention, intraoperative localization of lung nodules is still challenging in many cases. This is particulary true when the nodules to be resected are small, sub-solid or deep within the parenchyma.[7] The cause of this problem is the anatomical disparity between the intraoperative and preoperative configurations, as a consequence of large lung deformations present during surgery. These lung deformations can be mainly associated to two different sources: on the one hand, the patient position is changed from supine in preoperative CT acquisition to lateral decubitus in the operating room, which affects the way gravity influences internal organs. On the other hand, for the comfortable manipulation of the lung during surgery, the surgeon creates space inside the thoracic cage by allowing air getting into the intrapleural space. This phenomenon, known as a pneumothorax, produces a total collapse of the lung towards the mediastinum that modifies internal lung structures.

Corresponding author: pablo.alvarez@etudiant.univ-rennes1.fr

Medical Imaging 2018: Image-Guided Procedures, Robotic Interventions, and Modeling, edited by Baowei Fei, Robert J. Webster III, Proc. of SPIE Vol. 10576, 105761D · © 2018 SPIE
CCC code: 1605-7422/18/$18 · doi: 10.1117/12.2293938

Thanks to its low dose radiation and fast acquisition time, intraoperative Cone-Beam CT (CBCT) imaging could guide the localization of challenging nodules during a VATS intervention.[8,9] Nonetheless, lung structures are more difficult to see in CBCT images given the reduced image quality when compared to CT images. In addition, the intensity contrast between lung nodules and lung's parenchyma is decreased as a consequence of the deformation induced by the pneumothorax. In fact, the parenchyma becomes denser due to lung deflation. This is particularly problematic for the localization of low density lung nodules also referred as Ground Glass Opacities (GGO). A possible solution to this problem might be the superposition of preoperative CT information (*e.g.* segmentation of nodules and other important structures) with the intraoperative CBCT image, via an image registration procedure. However, the existence of large lung deformations makes such a task a real challenge.

This paper focuses on the quantification of the deformations induced by the change of the patient position between preoperative and intraoperative configurations during a VATS intervention. Understanding these deformations might be an important factor towards the development of an efficient image-guided surgery procedure. A non-rigid registration method is proposed for the superposition of preoperative CT and intraoperative CBCT lung structures. The resulting geometrical transformation is then used to quantify the deformations needed to achieve such superposition. To the best of our knowledge, no study has ever tried to quantify the lung deformations occurring during a VATS intervention, even before pneumothorax.

2. MATERIALS AND METHODS

2.1 Data

The work herein presented is a feasibility study performed on one clinical case only. In this context, a wedge resection was prescribed to the patient for a solitary nodule of approximately 13 millimeters in diameter. The VATS surgical intervention was done at the Rennes University Hospital, Rennes, France. This study was approved by the local ethics committee and the patient gave informed consent prior to the procedure.

The study consisted of the acquisition of two tomographic images: a preoperative CT, where the patient is in supine position and was instructed to hold his breath during the capture (end of inspiration cycle); and an intraoperative CBCT where the patient is in lateral decubitus position under sedation and mechanical ventilation. No surgical action was done before the CBCT acquisition, so that the patient's lung could be imaged in a fully inflated state, *i.e.* witouth pneumothorax.

Figure 1 shows an axial view of the images. Although the nodule is here clearly visible in both modalities, it is worth mentioning that it might not be the case, particularly for GGO nodules. While nodule visibility in intraoperative images plays an important role in image guided thoracic surgery, it is not relevant for the purposes of this work.

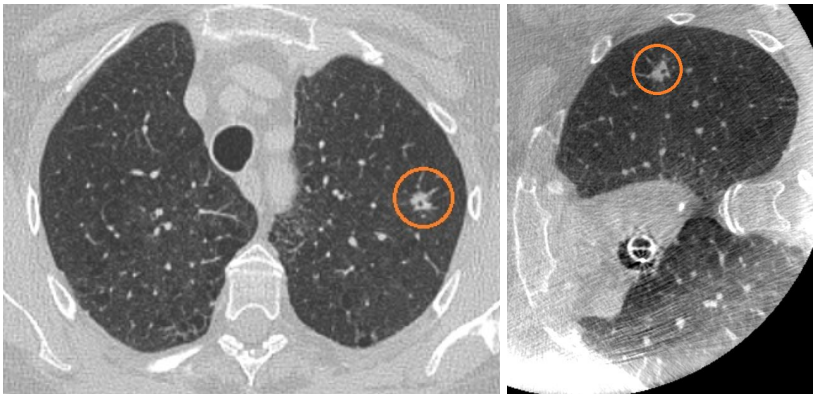

Figure 1. Slices in approximately the same transversal plane for preoperative CT (supine position) and intraoperative CBCT (lateral decubitus position). The nodule is encircled in orange. The change of configuration from preoperative to intraoperative configurations is clearly visible.

2.2 Segmentation

Segmentation of the lung parenchyma was achieved using an own modified version of Chest Imaging Platform, an open source library for image processing and analysis of chest CTs.[10] The method is based on a thresholding approach that exploits the differences in intensity of voxels inside and outside the lungs, which resulted in a segmentation containing both lungs and airways. A 3D Iterative Region Growing approach was used to segment only the primary airway branches, which were then removed from the previously obtained lung's segmentation. This allowed the separation of the two lungs, to extract the affected lung by using connected component analysis and *a priori* information on the position. Finally, morphological operations where applied to fill in holes and smooth irregular boundaries that were present mostly towards the mediastinum.

Given the reduced quality of the CBCT image, the aforementioned segmentation procedure was only used on the preoperative CT image. However, a similar approach using morphological eroding operations instead of airways extraction was applied to the CBCT to obtain a rough segmentation of the intraoperative lung. This latter is not accurate, and hence it is only used for the initialization of the registration workflow.

2.3 Registration

The registration process aims to account for lung deformations that occur after a change in patient position before and during a VATS intervention. A registration workflow composed of three steps is proposed: (1) initial alignment, (2) rigid registration and (3) non-rigid registration.

2.3.1 Initial alignment

As discussed before, preoperative and intraoperative images were taken under different configurations. Hence, the position of such images in the physical space is non-overlapping. To compensate for this misalignment, the centroids of the lung segmentations were superposed by translating the preoperative CT image. In addition, the change of orientation of the lung was assumed to be of approximately 90 degrees on the axial plane, so a rotation of this amount was also applied.

2.3.2 Rigid registration

Once the images were roughly aligned, an image-based rigid registration process was performed. The idea was to find a geometrical transformation that maximized image correspondence without introducing local deformations. This rigid registration step is of great importance since it affects directly the latter measurement of local deformations. Although different sources of information could be used to drive such registration (*e.g.* spine and ribs, airway tree, etc.), emphasis was made on structural information of the parenchyma. So, the optimization of a similarity metric estimated over the gray level information contained inside the lung mask was performed, disregarding the rest of the information on the image.

The procedure was accomplished using the multi-resolution image registration techniques implemented in the Elastix toolbox.[11] Normalized Mutual Information was used as a similarity metric, with an Adaptive Stochastic Gradient Descent optimization process. For each iteration, a set of 3000 paired random points were extracted inside the lung's segmentation and were used for the computation of the similarity metric. Several image resolutions were necessary to allow the algorithm to account for large displacements.

2.3.3 Non-rigid registration

The last step of the registration workflow consists of maximizing image correspondence by allowing local deformations. Any non-rigid registration procedure is characterized by the similarity metric, the optimization method and the elastic transformation model. For the first two components, as for the rigid registration step, the Normalized Mutual Information similarity metric estimated on samples over the lung's parenchyma, along with an Adaptive Stochastic Gradient Descent optimizer were used. B-Splines were chosen as the elastic transformation model. Over-deformation was avoided by restricting the degrees of freedom of the transformation, *i.e.* reducing the amount of control points. For that, a grid spacing of 16 mm in the highest resolution was chosen, which was found empirically to be large enough to allow fine deformations but also small enough to avoid over-registration. Elastix toolbox was again used to accomplish this task, by taking the rigidly registered image as the starting point.

3. RESULTS

An illustration of the qualitative results obtained after applying the proposed registration workflow is presented in Figure 2. Image misalignment is represented using a complementary color approach. After the initial alignment and rigid registration steps, there is an overall good overlap of the lung's parenchyma (left). This can be particularly appreciated towards the lateral and posterior parts of the lung contour. However, important misalignments still remain towards the medial and anterior parts of the lung, since they can not be recovered without allowing local deformations. These misalignments mainly disappear after the final non-rigid registration step (middle). The lung contours are now better matched and disparities on internal structures are recovered.

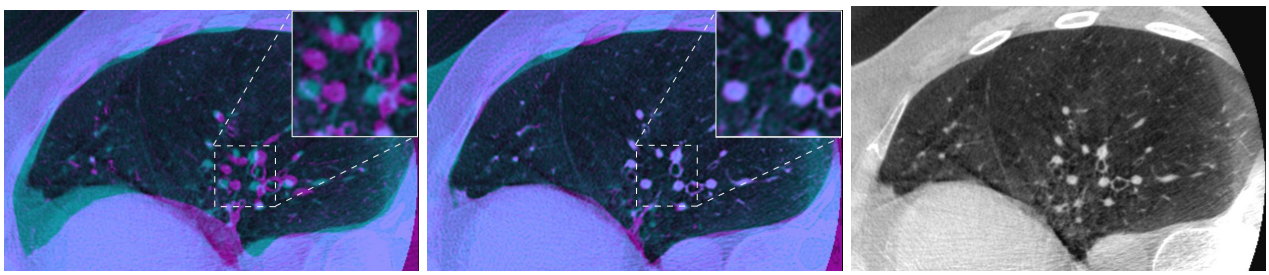

Figure 2. Axial view of the lung. Left: CT-CBCT image overlap after rigid registration. Middle: CT-CBCT image overlap after non-rigid registration. Right: target intraoperative CBCT image.

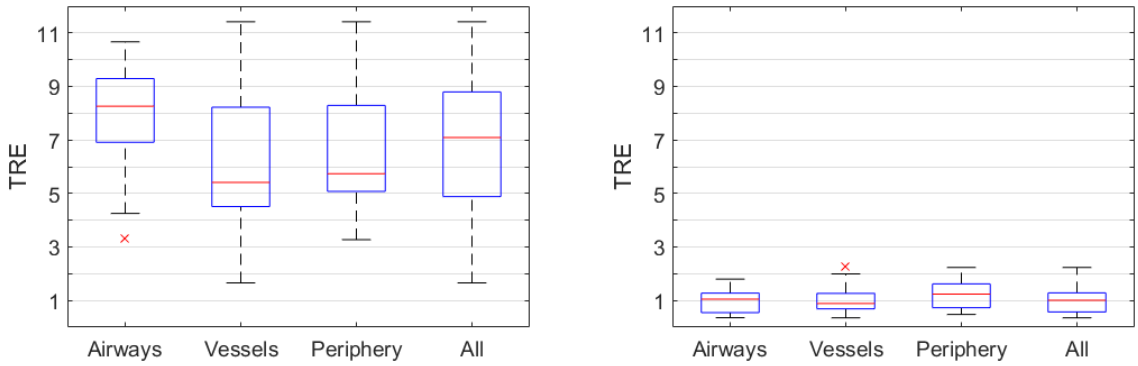

Figure 3. Target Registration Errors (TRE) in millimeters for different landmark groups before and after non-rigid registration.

Before the quantification of local lung deformations, a quantitative evaluation of the registration accuracy had to be performed. For that, the Target Registration Error (TRE) between a set of 51 paired anatomical landmarks was calculated. These landmarks were manually placed by an expert thoracic surgeon both in CT and CBCT, during a single session. Instructions were given so that the spatial distribution was as homogeneous as possible, covering the whole lung. Three landmark groups could be identified: 20 landmarks on airway bifurcations, 30 landmarks on vessel bifurcations and 14 landmarks towards the periphery of the lung, where the distance to the surface is lower than 18 mm. Additionally, another landmark was placed inside the nodule. Figure 3 presents the TREs obtained before and after the non-rigid registration procedure was applied.

The spatial distribution of the anatomical landmarks can be seen in Figure 4. Emphasis was given to the set of peripheral landmarks, which was the group where the remaining TREs were the highest. It is clear from the figure that misalignments of anatomical landmarks existing after rigid registration were successfully recovered after non-rigid registration, when local deformations of the lung were taken into account.

Finally, the magnitude of the deformation field obtained after non-rigid registration is depicted in Figure 5. Two anatomical planes are used to illustrate how such deformation is distributed throughout the parenchyma.

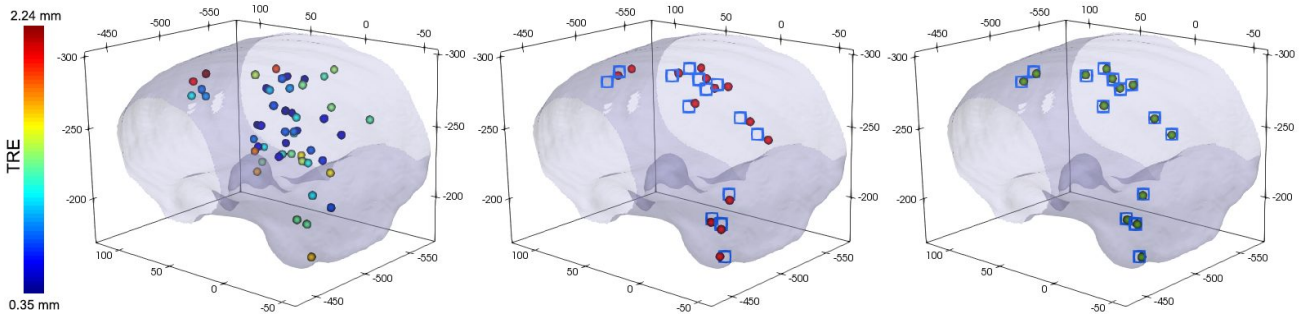

Figure 4. Spatial distribution of the whole set of landmarks. Left: Color map representation of the TREs after non-rigid registration, for all landmarks. Middle: Set of preoperative periphery landmarks (red spheres) after rigid registration compared to intraoperative periphery landmarks (blue squares). Right: Set of preoperative periphery landmarks (green spheres) after non-rigid registration compared to intraoperative periphery landmarks (blue squares).

In addition, the normalized histogram of deformations present on the whole lung volume is also presented.

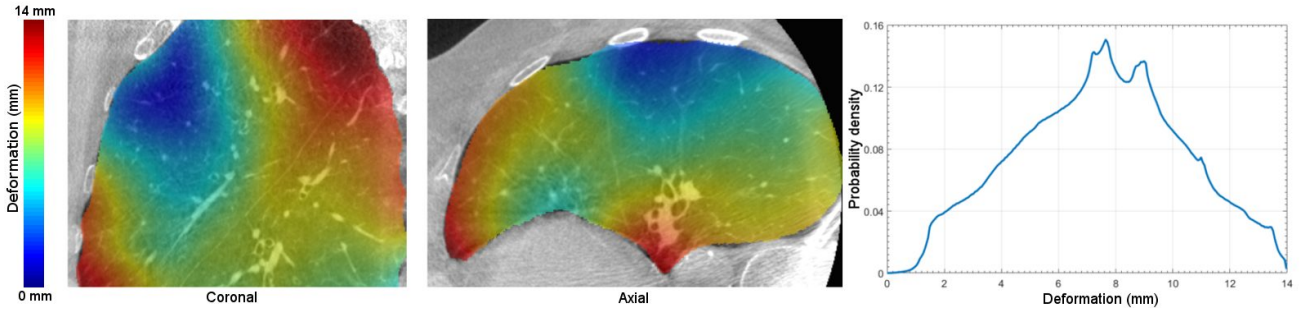

Figure 5. Left: color mapped local deformations in millimeters for coronal and axial views of the lung. Right: the normalized histogram of local deformations in millimeters for the whole lung volume.

4. DISCUSSION

As for the segmentation of the lung, the proposed procedure was straightforward on the preoperative CT and produced a smooth binary mask of the lung's parenchyma. For the CBCT, however, the reduced image quality did not allow the same results. The modified segmentation procedure was then applied, and even if it could not completely recover the whole lung structure, the result was sufficient to estimate the lung's centroid required for the initialization of the registration workflow.

With respect to image registration, the TREs obtained after rigid registration only where on the order of 7 mm, with better aligned landmarks near the vessels and lung periphery ($\sim$ 6 mm) than near the airways ($\sim$ 8 mm). A significant error reduction was achieved after non-rigid registration. In fact, median values of TREs for all landmark groups where reduced to 0.44 mm, 0.89 mm and 1.24 mm for airways, vessels and peripheral landmarks, respectively. In particular, a TRE reduction from 7.3 mm to 0.4 mm was observed for the the landmark placed inside the nodule. It is important to note that after non-rigid registration, the largest TREs are located in the lung's periphery. Lung structures are the smallest in this regions, hence Partial Volume Effects (PVE) in the image are more important. As a result, the registration algorithm has more trouble finding correspondences, which produces larger misalignments. Overall, a median TRE of 1.01 mm was obtained for the whole set of landmarks after non-rigid registration, with a minimum of 0.35 mm and a maximum of 2.24 mm. Since the majority of the TREs are around 1.01 mm (see Figure 3), one can conclude that the resulting registration is accurate, since the errors are on the order of image spacing.

Regarding the magnitude of the deformations, experimental results showed non-negligible measurements with maximum values around 14 mm, in different areas. However, a special remark has to be made with respect to the anatomical interpretation of these deformations' locations. Although the measured deformations were here

the highest near the apex and anterior parts of the lung (see Figure 5), this does not necessarily mean that these regions are the most affected by the change of configuration before the VATS intervention. In fact, the measurement of local deformations is highly sensitive to the initial alignment and rigid registration steps: a minimization of these local deformations in some regions of the lung will necessarily result in an increase in others. Hence, since there is anatomically no fixed point in the chest, deformations between the lung's areas are always relative. Other results would have been obtained with different initial geometrical transformations. However, the relative differences would remain similar.

To conclude, it is clear that important, non-uniform deformations of the lung occur between the pre- and intraoperative configurations. They are caused by a change of the patient pose, breathing mechanics and how gravity affects internal structures. Only a non-rigid registration procedure can cope with these local deformations, to obtain a perfect match between preoperative CT and intraoperative CBCT images.

5. CONCLUSION

This paper presents a registration workflow that was used to measure lung deformations resulting from changes between preoperative and intraoperative configurations during a VATS intervention. Registration accuracy was measured using TREs on a set of 51 paired anatomical landmarks, obtaining a median error of 7.09 mm after rigid registration, which was significantly reduced to 1.01 mm after non-rigid registration. Deformations throughout the lung where measured to be of maximum 14 mm ($\sim$ 7 mm in average) on different regions of the lung.

Experimental results highlighted the importance of accounting for lung deformations during VATS, since it will be necessary for transforming information extracted from preoperative images to the intraoperative setting. This will be of particular importance for the localization of lung nodules, which might be not visible through intraoperative imaging when their density or size is considerably low.

Future work includes the study of lung deformations on a dataset of several cases. Also, the analysis of the deformation under different rigid initialization approaches might be of interest for the identification of deformed lung regions. Finally, special focus must be brought to the correction of deformations induced by the pneumothorax that will allow the prediction of nodule displacement during VATS, which is the long-term goal of this work.

ACKNOWLEDGMENTS

The work presented in this article was partially supported by the *Région Bretagne* through its *Allocations de Recherche Doctorale* (ARED) framework and by the French National Research Agency (ANR) through the frameworks *Investissements d'Avenir Labex CAMI* (ANR-11-LABX-0004) and *Infrastructure d'Avenir en Biologie et Santé* (ANR-11-INBS-0006).

REFERENCES

[1] Jemal, A., Bray, F., Center, M. M., Ferlay, J., Ward, E., and Forman, D., "Global Cancer Statistics," *CA: A Cancer Journal for Clinicians* **61**, 69–90 (Mar. 2011).

[2] Stewart, B. W. and Wild, C. P., eds., [*World Cancer Report 2014*] (2014). OCLC: 903962851.

[3] Siegel, R. L., Miller, K. D., and Jemal, A., "Cancer Statistics, 2016," *CA: A Cancer Journal for Clinicians* **66**, 7–30 (Jan. 2016).

[4] Henschke, C. I., McCauley, D. I., Yankelevitz, D. F., Naidich, D. P., McGuinness, G., Miettinen, O. S., Libby, D. M., Pasmantier, M. W., Koizumi, J., Altorki, N. K., and others, "Early Lung Cancer Action Project: overall design and findings from baseline screening," *The Lancet* **354**(9173), 99–105 (1999).

[5] National Lung Screening Trial Research Team, Aberle, D. R., Adams, A. M., Berg, C. D., Black, W. C., Clapp, J. D., Fagerstrom, R. M., Gareen, I. F., Gatsonis, C., Marcus, P. M., and Sicks, J. D., "Reduced Lung-Cancer Mortality with Low-Dose Computed Tomographic Screening," *The New England Journal of Medicine* **365**, 395–409 (Aug. 2011).

[6] McKenna, R. J. and Houck, W. V., "New approaches to the minimally invasive treatment of lung cancer," *Current Opinion in Pulmonary Medicine* **11**, 282–286 (July 2005).

[7] Gould, M. K., Donington, J., Lynch, W. R., Mazzone, P. J., Midthun, D. E., Naidich, D. P., and Wiener, R. S., "Evaluation of Individuals With Pulmonary Nodules: When Is It Lung Cancer?," *Chest* **143**(5), e93S–e120S (2013).

[8] Uneri, A., Nithiananthan, S., Schafer, S., Otake, Y., Stayman, J. W., Kleinszig, G., Sussman, M. S., Prince, J. L., and Siewerdsen, J. H., "Deformable registration of the inflated and deflated lung in cone-beam CT-guided thoracic surgery: Initial investigation of a combined model-and image-driven approach," *Medical physics* **40**(1) (2013).

[9] Rouzé, S., de Latour, B., Flcher, E., Guihaire, J., Castro, M., Corre, R., Haigron, P., and Verhoye, J.-P., "Small pulmonary nodule localization with cone beam computed tomography during video-assisted thoracic surgery: a feasibility study," *Interactive CardioVascular and Thoracic Surgery* **22**, 705–711 (June 2016).

[10] Ross, J. C., Harmouche, R., Onieva, J., Diaz, A. A., and Washko, G. R., [*Chest Imaging Platform: An Open-Source Library and Workstation for Quantitative Chest Imaging*].

[11] Klein, S., Staring, M., Murphy, K., Viergever, M., and Pluim, J., "elastix: A Toolbox for Intensity-Based Medical Image Registration," *IEEE Transactions on Medical Imaging* **29**, 196–205 (Jan. 2010).